EasyChair Preprint

№ 9670

A Numerical Study on the Fluid Flow Through Two Tandem Circular Cylinders with Different Sizes Using the Lattice-Boltzmann Method

Van Tuyen Vu, Viet Dung Duong and Ich Long Ngo

February 5, 2023

A numerical study on the fluid flow through two tandem circular cylinders with different sizes using the Lattice-Boltzmann method

Van Tuyen Vu[1], Viet Dung Duong[2,*], and Ich Long Ngo[1,*]

[1] *School of Mechanical Engineering, Hanoi University of Science and Technology,*

No. 01, Dai Co Viet, Hai Ba Trung, Hanoi, Vietnam

[2] *School of Aerospace Engineering, University of Engineering and Technology,*

Vietnam National University, Ha Noi City, Vietnam

[*] Email: long.ngoich@hust.edu.vn

Abstract. This paper describes an investigation of fluid flow through two tandem circular cylinders using Lattice-Boltzmann Method in direct numerical simulation. The diameter ratio of two circular cylinders, D_1/D_2 varies from 0.5 to 1.5, and spacing ratio (L/D_2) varies from 1.5 to 10, whereas the Reynolds number of 100 is considered. The numerical model is well validated by comparing the results with those obtained in the literature. Flow regimes are observed, including two vortex shedding modes (two-layered and primary vortex). Furthermore, the flow characteristics depend significantly on the diameter ratio of two circular cylinders. The drag coefficient increases with an increase in D_1/D_2 while the Strouhal number generally decreases with increasing D_1/D_2. Additionally, the maximum C'_L obtained is at $L/D_2 = 5.0$. The results obtained are very useful for many applications, such as tube bundles of heat exchangers, offshore risers, and pipe racks.

Keywords: Computational fluid dynamic, Direct numerical simulation, Flow characteristic, Lattice Boltzmann method, Vortex flow

1. Introduction

The flow past the system of two or more cylinders is of concern in many engineering applications, including heat exchanger tubes, bundled transmission lines, buildings, and offshore risers. Naturally, the dynamics of flow past multiple closely separated cylindrical structures play an important role in fundamental and practical engineering due to the proximity effect. The effect classifies the flow around two tandem circular cylinders into the most generic flow features, such as shear layer separation/ reattachment, periodic vortex shedding, recirculation bubble, and vortex-vortex/ vortex-wall interaction. Therefore, the flow around two tandem circular cylinders provides an excellent model for extracting the flow physics of multiple cylindrical structures. The characteristics of this flow strongly depend on the cylinder spacing (L/D_2, where L is the spacing between upstream and downstream cylinders, and D_2 is the cylinder diameter of the downstream cylinder), the Reynolds number (Re) (based on D_2), and the ratio of cylinder diameters (D_1/D_2, where D_1 and D_2 are the diameters of the upstream and downstream cylinders, respectively). Although extensive investigations have been conducted to understand the dependence of the flow on L/D_2 and Re [1-8], the effect of D_1/D_2 is rarely investigated.

The wake flow of two tandem cylinders of identical diameter is classified by Igarashi [3,4] and Zdravkovich [2] into three regimes: (i) the extended-body regime ($0.5 < L/D_2 < 10$), (ii) the reattachment regime ($1.0 < L/D_2 < 3.5$), and the co-shedding regime ($L/D_2 > 3.5$). For the first regime, the shear layers separated from the upstream cylinder overshoot the downstream. While the separated shear layers reattach to the downstream cylinder in the second regime, both cylinders generate vortices at the identical frequency in the third regime. As reported by Igarashi [3], the critical spacing $(L/D_2)_c$ signifies the transition between the reattachment and co-shedding regimes, where both reattachment and co-shedding flows occur intermittently. Xu and Zhou [9] examined the Re effect on the flow classification

(Re = 0.8×10^3 – 4.2×10^4) and further divided the reattachment regime into two sub-regimes for L/D_2 = 1.5–2.5 and 2 – 4.5, corresponding to the occurrence of shear layer reattachment on the downstream and upstream sides of the downstream cylinder respectively (see also Zhou and Yiu [10]). Ljungkrona, Norberg and Sunden [6] and Ljungkrona and Sunden [11] found at Re = 0.33×10^4 – 4.9×10^4 that $(L/D_2)_c$ decreases with increasing Re because of the dependence of the vortex formation length on Re.

For the aerodynamic coefficients of two tandem cylinders of identical diameter, extensive investigations have been conducted (Zdravkovich [1], Igarashi [3,4], Arie et al. [5], Alam et al. [8], Ljungkrona and Sunden [11], Jendrzejcyk and Chen [12], Zhang and Melbourne [13], Alam and Zhou [14], Sumner [15], Alam [16,17]). The time-mean drag coefficient ($\bar{C}_D$) on the upstream cylinder gradually decreases with L/D_2 in the overshoot and reattachment regimes. On the other hand, $\bar{C}_D$ of the downstream cylinder is negative (forward thrust) for $L/D_2 < 3.5$, with a local maximum of $\bar{C}_D$ at $L/D_2 \approx 2$ (Zdravkovich and Pridden [1], Igarashi [3], Alam et al. [8]). The occurrence of the local maximum of $\bar{C}_D$ is Re-dependent. The local maximum of $\bar{C}_D$ appears for Re > 3.1×10^4 and disappears for Re < 3.1×10^4. Alam [16] discussed the physical aspects behind the presence and absence of the local maximum of $\bar{C}_D$. The fluctuating drags and lift coefficients, C'_D and C'_L of the downstream cylinder are much larger than those of the upstream cylinder in the reattachment and co-shedding regimes; and they are strongly dependent on L/D_2 in the reattachment regime (Alam et al. [8]). Furthermore, the Strouhal number (St) characterizes the wake of two tandem cylinders. It is now well documented that the two cylinders shed vortices at the same frequency at least up to L/D_2 = 10.0, and two distinct values of St occur only in the transition from one regime to another (Igarashi [3,4], Alam et al. [8], Novak [18], Kiya et al. [19], Xu and Zhou [20]). The flow structure has been characterized by Sumner [15], Yiu, Zhou and Zhu [20] and Zhou and Yiu [22] and Zhou and Alam [23] give recent reviews of past investigations of flow past multiple cylinders with identical diameters.

Previous investigations have greatly improved our understanding of the fluid dynamics around two tandem cylinders of identical diameters. However, the engineering structures in a group or proximity are not always of the same diameter. For example, an offshore piggyback pipeline normally comprises one small pipe and a large pipe (either in contact or separated depending on the design and installation requirements). Also, there have been so far few investigations on the wake of two tandem cylinders of different diameters. To investigate the feasibility of flow control, Lee and Park [24] measured $\bar{C}_D$ on the downstream cylinder when placing a small control cylinder upstream (L/D_2 = 3.75 – 26.25, D_1/D_2 = 0.133 – 0.276, Re = 2.0×10^4). They observed a maximum reduction in $\bar{C}_D$ by 29% at D_1/D_2 = 0.233 and L/D_2 = 6.786. Zhao et al. [25] performed a numerical simulation of the wake flow through two different cylinders (D_1/D_2 = 0.25) at Re = 500 and showed that the gap between cylinders had a significant effect on the forces on the downstream cylinder, and its increase from $0.05D_2$ to $1.0D_2$ was followed by a decrease in $\bar{C}_D$. Zhao et al. [26] performed a similar numerical investigation at Re = 5.0×10^4 for D_1/D_2 = 0.5 with a gap of $0.05D_2$ – $0.4D_2$ and found that $\bar{C}_D$ was almost independent of the gap size. Alam and Zhou [14] conducted a detailed experimental investigation on the wake of two tandem cylinders of different diameters (D_1/D_2 = 0.24 – 1.0) at a fixed L/D_2(= 5.5). They made an interesting finding, that is, two predominant frequencies were detected behind the two cylinders, one identical to that of the vortex shedding from the upstream cylinder and the other from the downstream cylinder being lower. They further found that D_1/D_2 may have a pronounced effect on the time-averaged and fluctuating forces on the downstream cylinder.

The previous scattered investigations naturally cannot provide the full picture of the wake of two tandem cylinders of different diameters and many issues have yet to be resolved. For instance, how does the flow structure change as L/D_2 varies in a wider range from 1.0 to 10 and D_1/D_2 exceeds 1.0? Is it followed by drastic changes in the fluid forces on the downstream cylinder? How is the frequency of vortex shedding from the downstream cylinder influenced by that from the upstream one at $D_1/D_2 > 1.0$? How should the flow regimes be classified? What are the fluid dynamics characteristics compared

with those associated with two identical cylinders? This work aims to cope with these issues. The flow structure of two tandem circular cylinders, predominant vortex shedding frequencies along with $\bar{C}_D$, C'_D, C'_L, and *St*, are all investigated as L/D_2 and D_1/D_2 are respectively varied in ranges of 1.5 – 10 and 0.5 – 1.5 at Re =100, which cover all possible changes in the flow structure. This low Reynolds number eliminates the turbulence caused by flow distortion, thus ensuring physically two-dimensional vortex dynamics (Vorobieff et al. [27]).

2. Governing equation and numerical methods

2.1. Lattice Boltzmann method for incompressible flows

The LBM is a mesoscopic dynamics-based technique. The fluid flow is made from a collection of pseudo-particles. On a discrete lattice grid, these particles perform constant streaming and collision. In this study, the particle's velocity is discretized to nine velocity vectors $\boldsymbol{c}_i$ at two-dimensional lattice locations. This velocity set known name the D2Q9 model. The vectors of velocity are:

$$\boldsymbol{c}_i = \begin{cases} (0,0) & i = 0 \\ (0,\pm 1)c,\ (\pm 1,0)c & i = 1,2,3,4 \\ (\pm 1,\pm 1)c & i = 5,6,7,8 \end{cases} \tag{1}$$

where $c = \Delta x/\Delta t$ represents the lattice seed, Δx is the lattice length, and Δt is the constant time step. The most important variable in the LBM is the particle distribution function $f_i(\boldsymbol{x}, t)$(PDF), which indicates the chance of meeting a particle with a velocity $\boldsymbol{c}_i$ at spatial point x and time t. The state of the fluid is updated by computing the particle distribution function using the discrete Boltzmann equation shown below:

$$f_i(\boldsymbol{x} + \boldsymbol{c}_i \Delta t, t + \Delta t) = f_i(\boldsymbol{x}, t) - \frac{\Delta t}{\tau}\left[f_i(\boldsymbol{x}, t) - f_i^{eq}(\boldsymbol{x}, t) \right] \tag{2}$$

Here, the Bhatnagar-Gross-Krook collision model [17] with a single relaxation time is used and τ denotes the relaxation time. The term $f_i^{eq}(\boldsymbol{x}, t)$ represents the equilibrium distribution function, which has the following formula:

$$f_i^{eq} = \rho w_i \left[1 + 3c \cdot \boldsymbol{u} + \frac{9}{2}(c \cdot \boldsymbol{u})^2 - \frac{3}{2}\boldsymbol{u} \cdot \boldsymbol{u} \right] \tag{3}$$

where $w_0 = 4/9, w_{1-4} = 1/9$ and $w_{5-8} = 1/36$ for D2Q9 lattice. $\rho(\boldsymbol{x}, t)$ and $\boldsymbol{u}(\boldsymbol{x}, t)$ denote the density and velocity of the macroscopic fluid, which may be computed using the following equations:

$$\rho = \sum_i f_i,\ \rho \boldsymbol{u} = \sum_i c_i f_i \tag{4}$$

The kinematic viscosity is linked to the relaxation time by the following formula:

$$\nu = c_s^2 \left(\tau - \Delta t/2 \right) \tag{5}$$

where c_s is the lattice sound speed. The pressure field may be calculated using the state equation for an ideal gas, $p = \rho c_s^2$. The global hydrodynamic coefficients, such as lift and drag coefficients, pressure coefficient, Strouhal number, mean drag coefficient, and root-mean-square value of lift coefficient, are accordingly computed as

$$C_D = \frac{F_x}{\frac{1}{2}\rho U_\infty^2 D_2},\quad C_L = \frac{F_y}{\frac{1}{2}\rho U_\infty^2 D_2},\quad C_P = \frac{p - p_\infty}{\frac{1}{2}\rho U_\infty^2},\quad St = \frac{f \cdot D_2}{U_\infty}, \tag{6}$$

$$\bar{C}_D = \frac{1}{N}\sum_{1}^{N} C_D, \quad C'_L = \sqrt{\frac{1}{N}\sum_{1}^{N}\left(C_L - \bar{C}_L\right)^2} \tag{7}$$

2.2. Numerical method

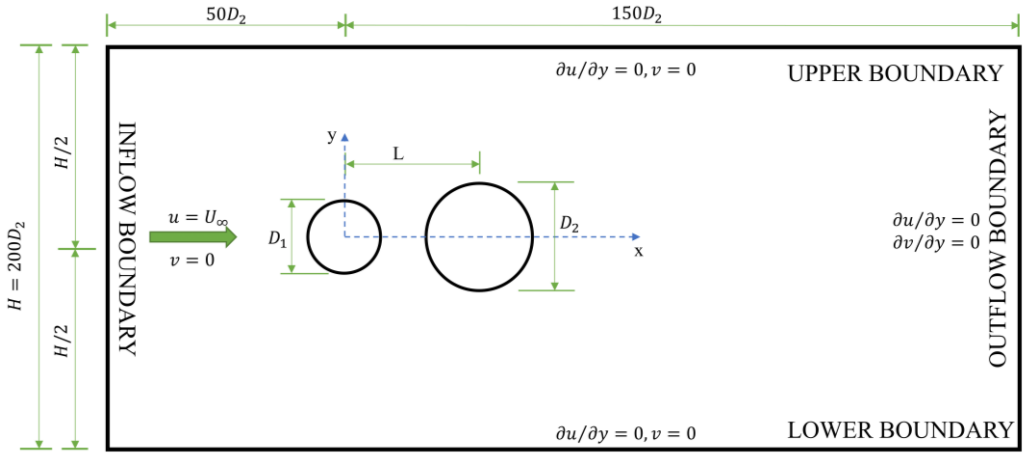

Figure 1. Schematic of the numerical model and boundary conditions.

The numerical model and boundary conditions are illustrated in Fig. 1. In this figure, the upstream cylinder is isolated at the coordinate origin and the downstream is simultaneously changed to ensure identical spacing (L) between them. In this study, the domain of computational is $200D_2 \times 200D_2$, that domain is big enough to ignore the effect of the wall on two cylinders. Following [16], the blockage ratio $B = D/H$, where H is the width of the computational domain) is required at 0.6% and the blockage ratio of this study is 0.5%, which is lower than the blockage ratio threshold. The inflow and outflow boundaries for the setup of boundary conditions are set up using Dirichlet-type and Neumann-type boundary conditions, respectively. The upper and lower boundaries are set as free-slip.

Table 1. Comparison of flow past a single circular cylinder at Re = 50, 100, 150, and 200.

Re	Authors	$\bar{C}_D$	C'_L	St
50	Qu et al. [31]	1.397	0.039	0.124
	Chen et al. [29]	1.427	0.039	0.123
	Present	1.426	0.039	0.127
100	Williamson [32]	-	-	0.164
	Chen et al. [29]	1.337	0.23	0.163
	Present	1.335	0.221	0.168
150	Qu et al. [31]	1.306	0.355	0.184
	Chen et al. [29]	1.316	0.363	0.181
	Present	1.316	0.359	0.184
200	Qu et al. [31]	1.32	0.457	0.196
	Chen et al. [29]	1.324	0.474	0.194
	Present	1.325	0.475	0.201

The mesh convergence was also tested to choose a fairly good grid resolution by selecting block level and cells [28]. Following that, the test uses four meshes and chooses the mesh have results are less than 1%. The mesh is performed corresponding to $y^+ = 0.085$, block level and cells are $6/12^2$. In this paper, the numerical algorithm is validated for a single circular cylinder at Re = 50–200 (Table 1) [28]. It compares well with the results of the hydrodynamic coefficient of Chen et al. [29], Qu et al. [31], and

Williamson [32], namely the minimum error is 0.07% and the maximum error is 4%.

3. Results and discussions

3.1. Flow classification

Three distinct flow regimes are identified for the flow past two tandem circular cylinders. These flow regimes were named overshoot ($1.0 < L/D_2 < 2.0$), reattachment ($2.0 < L/D_2 < 3.5$), and co-shedding ($L/D_2 > 3.5$). In the co-shedding regime, while the upstream cylinder always exhibits primary vortex shedding mode, two-layered and secondary vortex shedding modes are observed behind the middle cylinder for $3.5 < L/D_2 < 6.5$ and $6.5 < L/D_2 < 10.0$, respectively Zhu et al. [33].

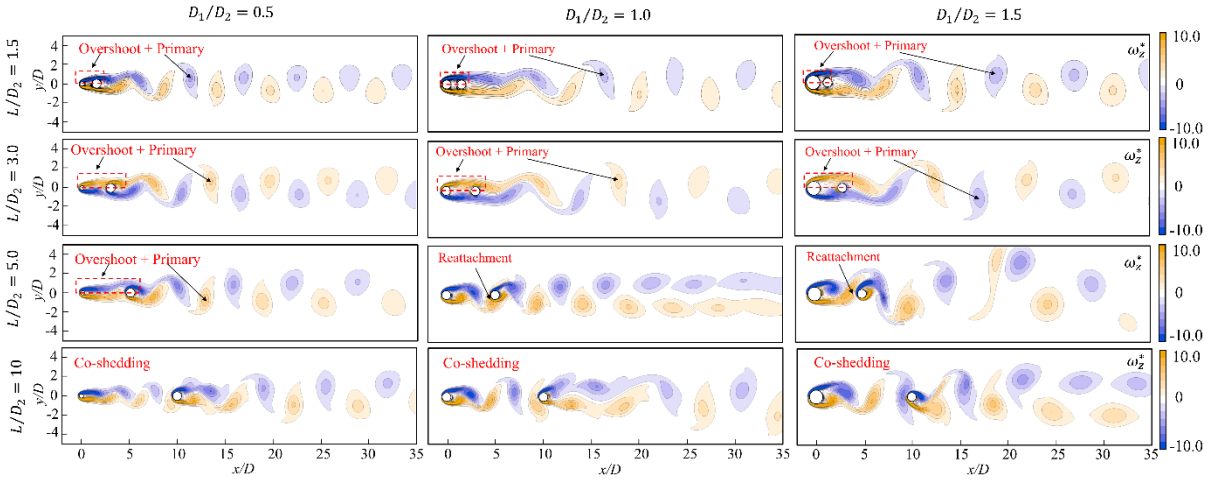

Figure 2. Classification of flow structures of two tandem circular cylinders with different sizes. The sequence of instantaneous normalized vorticity contours $\omega_z^*=\omega_z D/U_\infty$

The first and third modes show staggered counterrotating vortices; while the second mode presents two parallel vortex layers, where each layer is distributed by detectable individual vortices of the same sign. In this section, the flow characteristics of two tandem circular cylinders are discussed in the range of $D_1/D_2 = 0.5 - 1$ at Re = 100. Fig. 2 illustrates the flow structure classification of wake interference at representative spacing and diameter ratios. The wake structures are classified into four regimes: overshoot and primary, reattachment, and co-shedding. The details of the effect of these regimes on the hydrodynamic coefficients are produced in the following subsections.

3.2. Hydrodynamic coefficients and Strouhal numbers

Fig. 3 presents the hydrodynamic coefficients and Strouhal number of upstream and downstream cylinders. To highlight the proximity effect and diameter ratio effect, these coefficients of two tandem circular cylinders are compared with those of the single circular cylinder obtained in the previous section. The time-mean drag coefficient results of the upstream cylinder at four spacing ratios linearly increase with an increase in diameter ratio, while the higher L/D_2 shows the higher $\bar{C}_D$. At $D_1/D_2 = 1$, the $\bar{C}_D$ of the upstream cylinder at a large spacing ratio of $L/D_2 = 10$ approaches that of a single cylinder, confirming that at a sufficiently large spacing ratio there is no effect on the downstream cylinder. It is identical to what is observed in C'_L and *St* figures, except that the *St* decrease with an increase in D_1/D_2. The *St* decrease of the upstream cylinder interprets that the increase in diameter of the upstream cylinder modifies the vortex shedding from high to low frequency.

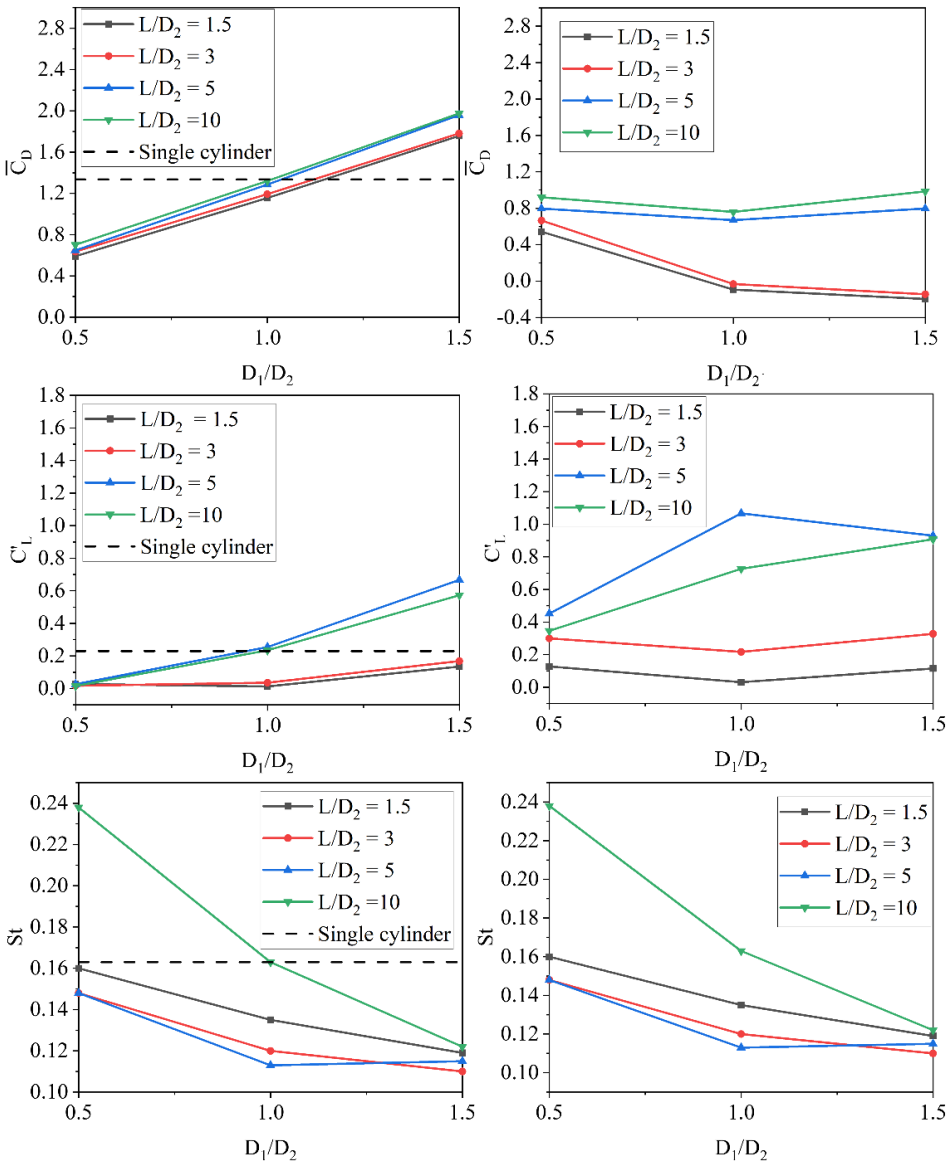

Figure 3. The variations of $\bar{C}_D$, C'_L, St with D_1/D_2 for two tandem circular cylinders with different sizes, the hydrodynamic coefficients and Strouhal number of the upstream cylinder ((left) and the downstream cylinder (right).

Additionally, the variation of the upstream cylinder plays a crucial role in reducing the $\bar{C}_D$ of the downstream cylinder, being lower than that of the single cylinder at every diameter ratio changing from 0.5 to 1.5. It is interesting to note that the C'_L of the downstream cylinder does not change significantly with an increase in D_1/D_2 at sufficiently small spacing ratios (L/D_2 = 1.5 and 3.0); while at sufficiently large spacing ratios (L/D_2 = 5.0 and 10.0), the C'_L of downstream cylinder dramatically increase with an increase of D_1/D_2 from 0.5 to 1.0. The maximum value of C'_L obtained is at L/D_2 = 5.0. This phenomenon is essential due to the interaction of the fluid flow through two cylinders. At small L/D_2, these two cylinders are close to each other, thus the synergic effect is strong. It means the flow through the upstream cylinders significantly affects the downstream cylinder and vice versa. In addition, the flow can pass through both cylinders, as shown in Fig. 2, L/D_2 = 1.5. In this regard, most streamlines do not cover the profile of two cylinders, and thus the hydrodynamic loss is high. As a result, the hydrodynamic coefficients including C'_L are low. However, the quality of the streamline increases with increasing L/D_2.

It means the flow can cover the cylinder profile, as illustrated in Fig. 2, L/D_2 = 3.0. Therefore, the hydrodynamic loss is lower, hence the C'_L increases accordingly. C'_L reaches its maximum value when the distance between two cylinders is far enough, e.g., L/D_2 = 5.0. At this point, the hydrodynamic loss is still low. If L/D_2 keeps increasing, the synergic effect becomes weak, and the hydrodynamic loss is no longer low due to the reduction in vortex intensity of the flow before reaching the downstream cylinder, as shown in Fig. 2, L/D_2 = 10. Consequently, C'_L intends to decrease accordingly. Additionally, the upstream flow still affects the downstream, thus the decrease of C'_L is more obvious, particularly for the downstream cylinder, as shown in Fig. 3 for C'_L (right). Fig. 3 also shows the *St* of the downstream cylinder is identical to that of the upstream cylinder. Noted that the same dominant wake structure of the Karman vortex is acting on both cylinders at every spacing and diameter ratio.

4. Conclusion

The flow around two circular cylinders with different diameters in tandem arrangements was numerically conducted by using lattice Boltzmann. The validations of the results were performed for isolated circular cylinders. The research points aim at the effects of cylinder spacing ratio and diameter ratio on the underlying fluid dynamics, including wake structures and hydrodynamics coefficients. The wake structures are classified into four regimes: overshoot and primary, reattachment, and co-shedding.

For the upstream cylinder, the time-mean drag coefficient results of the upstream cylinder at four spacing ratios linearly increase with an increase in diameter ratio, while the higher L/D_2 shows the higher $\bar{C}_D$. At D_1/D_2 = 1, the $\bar{C}_D$ of the upstream cylinder at a large spacing ratio of L/D_2 = 10 approaches that of a single cylinder, confirming that at a sufficiently large spacing ratio there is no effect of the downstream cylinder. It is identical to what is observed in C'_L and *St*, except that the *St* decrease with an increase in D_1/D_2. The *St* decrease of the upstream cylinder interprets that the increase in diameter of the upstream cylinder modifies the vortex shedding from high to low frequency.

For the downstream cylinder, the variation of the upstream cylinder plays a crucial role in reducing the $\bar{C}_D$ of the downstream cylinder, being lower than that of the single cylinder at every diameter ratio changing from 0.5 to 1.5. It is interesting to note that the C'_L of the downstream cylinder does not change significantly with an increase in D_1/D_2 at sufficiently small spacing ratios (L/D_2 = 1.5 and 3.0); while at sufficiently large spacing ratios (L/D_2 = 5.0 and 10.0), the C'_L of downstream cylinder dramatically increases with an increase of D_1/D_2 from 0.5 to 1.0. The maximum value of C'_L obtained is at L/D_2 = 5.0. The *St* of the downstream cylinder is identical to that of the upstream cylinder, notifying that the same dominant wake structure of the Karman vortex is acting on both cylinders at every spacing and diameter ratio.

Acknowledgments

This research is funded by the Hanoi University of Science and Technology (HUST) under project number T2022-PC-017.

References

[1] Zdravkovich, M. M. Review of flow interference between two circular cylinders in various arrangements. *Trans. ASME J. Fluids Eng*, **99**, (1977), pp. 618–633.
[2] Zdravkovich, M. M. The effects of interference between circular cylinders in cross flow. *J. Fluids Struct*, **1**, (1987), pp. 239–261.
[3] Igarashi, T. Characteristics of the flow around two circular cylinders arranged in tandem, 1st report. *Bull. JSME*, **24**, (1981), pp. 323–331.
[4] Igarashi, T. Characteristics of the flow around two circular cylinders arranged in tandem, 2nd report. *Bull. JSME* **27**, (1984), pp. 2380–2387.
[5] Arie, M., K Iya , M., Moriya , M. and Mori , H. Pressure fluctuations on the surface at two circular cylinders in tandem arrangement. *Trans. ASME J. Fluids Engng*, **105**, (1983), pp. 161–166.

[6] Ljungkrona. M, Norberg. C and Sunden. B. Free-stream turbulence and tube spacing effects on surface pressure fluctuations for two tubes in an in-line arrangement. *J. Fluids Struct*, **5**, (1991), pp. 701–727.
[7] Mahir. N. and Rockwell. D. Vortex formation from a forced system of two cylinders. Part 1. Tandem arrangement. *J. Fluid Mech*, **10**, (1996), pp. 473–489.
[8] Alam, M. M., Moriya. M., Takai , K. and Sakamoto, H. Fluctuating fluid forces acting on two circular cylinders in a tandem arrangement at a subcritical Reynolds number. *J. Wind Engng Ind. Aerodyn*, **91**, (2003), pp.139–154
[9] Xu, G. and Zhou , Y. Strouhal numbers in the wake of two inline cylinders. *Exp. Fluids* **37**, (2004), pp. 248–256.
[10] Zhou, Y. and Yiu , M. W. Flow structure, momentum and heat transport in a two-tandem-cylinder wake. *J. Fluid Mech*, **548**, (2006), pp. 17–48.
[11] Ljungkrona, L. and Sunden , B. Flow visualization and surface pressure measurement on two tubes in an inline arrangement. *Exp. Therm. Fluid Sci*, **6**, (1993), pp. 15–27.
[12] Jendrzejcyk, J. A. and Chen , S. S. Fluid forces on two circular cylinders in crossflow. *In Proceedings of the Flow-Induced Vibration*, **104**, (1986) pp. 1–13.
[13] Zhang, H. and Melbourne , W. H. Interference between two circular cylinders in tandem in turbulent flow. *J. Wind Engng Ind. Aerodyn*, **41–44**, (1992), pp. 589–600.
[14] Alam, M. M. and Zhou , Y. Strouhal numbers, forces and flow structures around two tandem cylinders of different diameters. *J. Fluids Struct*, **24**, (2008), pp. 505–524.
[15] Sumner, D. Two circular cylinders in cross-flow: a review. *J. Fluids Struct*, **26**, (2010), pp. 849–899.
[16] Alam, M. M. The aerodynamics of a cylinder submerged in the wake of another. *J. Fluids Struct*, **51**, (2014), pp. 393–400.
[17] Alam , M. M. Lift forces induced by the phase lag between the vortex sheddings from two tandem bluff bodies. *J. Fluids Struct*, **65**, (2016), pp. 217–237.
[18] Novak, J. Strouhal number of a square prism, angle iron and two circular cylinders arranged in tandem. *Acta. Tech. Czech. Acad. Sci*, **3**, (1974), pp. 361–373.
[19] Kiya, M., Arie , M., Tamura , H. and M Ori , H. Vortex shedding from two circulars in staggered arrangement. *J. Fluids Engng*, **102**, (1980), pp. 166–173.
[20] Xu, G. and Zhou , Y. Strouhal numbers in the wake of two inline cylinders. *Exp. Fluids*, **37**, (2004), pp. 248–256.
[21] Yiu, M. W., Zhou , Y. and Zhu , Y. G. Passive scalar transport in a turbulent cylinder wake in the presence of a the downstream cylinder. *Flow Turbul. Combust*, **72**, (2004), pp. 449–461.
[22] Zhou, Y. and Yiu , M.W. Flow structure, momentum and heat transport in a two-tandem-cylinder wake. *J. Fluid Mech*, **548**, (2006), pp. 17–48.
[23] Zhou, Y. and Alam , M. M. Wake of two interacting circular cylinders: a review. *Intl J. Heat Mass Transfer*, **62**, (2016), pp. 510–537.
[24] Lee, S. J., Lee , S. I. and Park , C. W. Reducing the drag on a circular cylinder by the upstream installation of a small control rod. *Fluid Dyn. Res*, **34**, (*2004*), pp. 233–250.
[25] Zhao, M., Cheng , L., T Eng , B. and Liang , D. Numerical simulation of viscous flow past two circular cylinders of different diameters. *Appl. Ocean Res*, **27**, (2005), pp. 39–55.
[26] Zhao, M., Cheng , L., Teng , B. and Dong , G. Hydrodynamic forces on dual cylinders of different diameters in steady current. *J. Fluids Struct*, **23**, (2007), pp. 59–83.
[27] Vorobieff, Peter, Daniel Georgiev, and Marc S. Ingber. Onset of the second wake: dependence on the Reynolds number. *Physics of Fluids*, **14**, (2002), pp. 53-56.
[28] Viet Dung Duong, Van Duc Nguyen, Van Tien Nguyen, et al. Low-Reynolds-number wake of three tandem elliptic cylinders, *Phys. Fluids*, **34**, (2022), pp. 043605(1)-043605-(23).
[29] S. Chen and G. D. Doolen, Lattice Boltzmann method for fluid flows, *Annu. Rev. Fluid Mech*, **30**(1), (1998), pp. 329–364.
[30] D. Yu, R. Mei, L.-S. Luo, and W. Shyy, Viscous flow computations with the method of lattice Boltzmann equation, *Prog. Aerosp. Sci*, **39**(5), (2003), pp. 329–367.
[31] L. Qu, C. Norberg, L. Davidson, S.-H. Peng, and F. Wang, Quantitative numerical analysis of flow past a circular cylinder at Reynolds number between 50 and 200, *J. Fluids Struct*, **39**, (2013), pp. 347–370.
[32] C. H. Williamson, Oblique and parallel modes of vortex shedding in the wake of a circular cylinder at low Reynolds numbers, *J. Fluid Mech*, **206**, (1989), pp. 579–627.
[33] Zhu, Hongjun, Jiawen Zhong, and Tongming Zhou. Wake structure characteristics of three tandem circular cylinders at a low Reynolds number of 160. *Physics of Fluids*, **33**, (2021), pp. 044113(1)-044113(19).